Understanding Fluorometric Interactions in Ion-Responsive Sustainable Polymer Nanocomposite Scaffolds

Shriram Janghela[a,b], Sudeepa Devi[a], Neelu Kambo[b], Debmalya Roy[a*], N. Eswara Prasad[c]

[a.] Directorate of Nanomaterials and Technologies, DMSRDE, GT Road, Kanpur, India-13
[b.] DMSRDE, GT Road, Kanpur, India-208013.

Data sheets-PU &PAN

Typical Properties* For Natural Resin	ASTM Test Method (Other)	Units U.S. Conventional	Units SI Metric	Texin SUN-3006 U.S. Conventional	Texin SUN-3006 SI Metric
General					
Specific Gravity	D 792 (ISO 1183)			1.08	
Shore Hardness	D 2240 (ISO 868)	A Scale		90	
Mold Shrinkage at 100-mil Thickness:	D 955 (ISO 2577)				
Flow Direction		in/in (mm/mm)		0.008	
Cross-Flow Direction		in/in (mm/mm)		0.008	
Water Absorption	D 570 (ISO 62)	%		1.3	
Light Transmission (350-1050 nm)	D 1003 (ISO 3538)	%		92.8	
Refractive Index	D 542 (ISO 489)			1.503	
Mechanical					
Tensile Strength	D 882	lb/in²	MPa	4,100	28.3
Ultimate Elongation	D 882	%		370	
Tear Strength, Die "C"	D 1004	lbf/in	kN/m	440	95
Thermal					
Glass Transition Temperature (Tg)	(DMA)[a]	°F	°C	-40	-40
Softening Temperature	(TMA)[b]	°F	°C	228	109

*These values are provided as general information only. They are approximate values and are not part of the product specifications.
[a] Dynamic Mechanical Analysis
[b] Thermal Mechanical Analysis

SIGMA-ALDRICH®

sigma-aldrich.com

3050 Spruce Street, Saint Louis, MO 63103, USA
Website: www.sigmaaldrich.com
Email USA: techserv@sial.com
Outside USA: eurtechserv@sial.com

Product Specification

Product Name:
Polyacrylonitrile - average M_W 150,000 (Typical)

Product Number:	181315
CAS Number:	25014-41-9
MDL:	MFCD00084395
Formula:	C3H3N

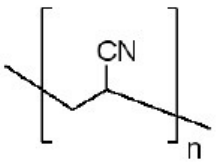

TEST	Specification
Appearance (Color)	White to Yellow
Appearance (Form) Powder and Chunks	Conforms to Requirements
Infrared spectrum	Conforms to Structure

Fig S1: The data sheet of Texin SUN 3006 polyurethane (upper) and polyacrylonitrile (lower) provided by Covestro, India and Sigma Aldrich respectively.

Schematic and representative images of different low dimensional carbonaceous nanomaterials

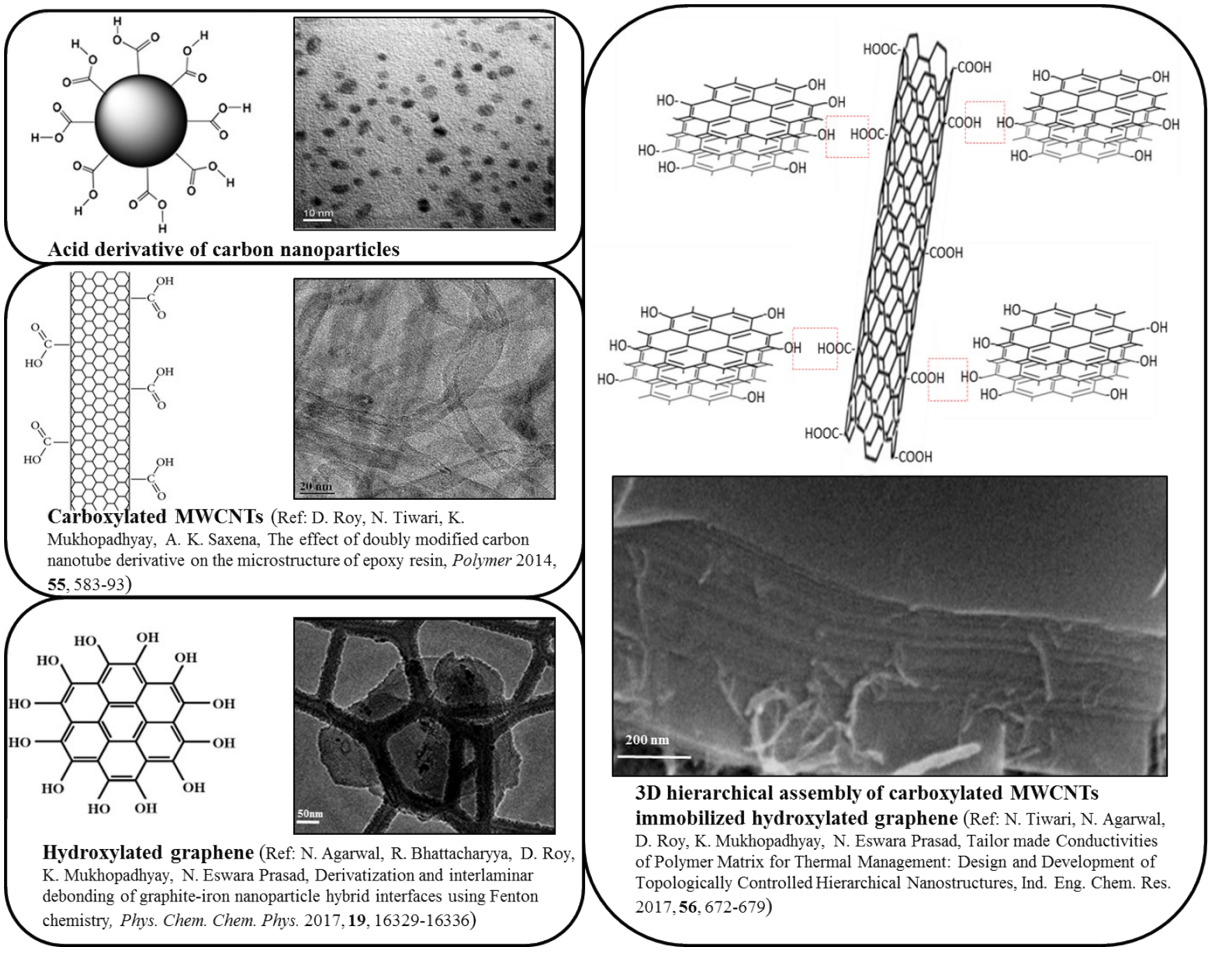

Fig S2: Schematic representation of different low dimensional functional carbon-based nanomaterials selected in this study.

Fluorescence images of before and after dichromate treatment of pristine and nanocomposite of polyurethane and polyacrylonitrile

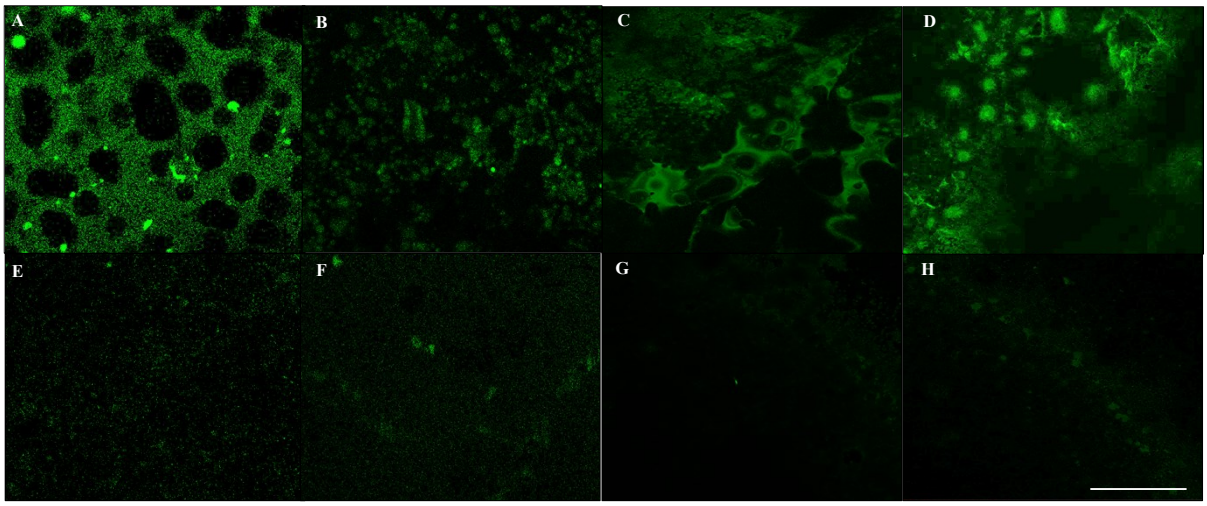

Fig S3: Fluorescence images of before (A, C & E, H') and after (B, D & F, H) metal ions treatment in pristine TPU (C, D), nanocomposite TPU (A, B), pristine PAN (G, H) and nanocomposite PAN (E, F) respectively. The samples were dried and fixed on a glass slide with a drop of epoxy glue and viewed under a epi-fluorescence microscope by excitation at 488 nm where the scale bar is 50 μm.

Dynamic Mechanical Analysis studies of PU and PU nanocomposite of 01 weight percentage of hybrid nanofillers

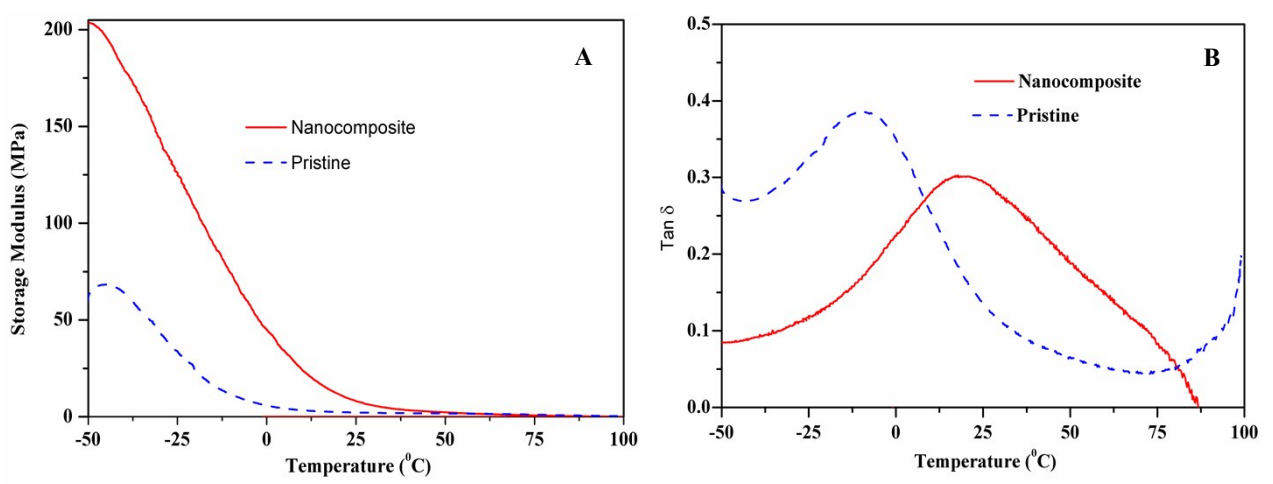

Fig S4: Dynamic Mechanical Analysis (DMA) studies of storage modulus (A) and glass transition temperature (B) of polyurethane matrix (blue dashed line) by addition of 01 weight percentage of hybrid nanofillers (red solid line) from -50 to 100^{0}C in tension mode with an oscillatory frequency of 1 Hz at a heating rate of 05^{0}C/min.

Transmission Electron Microscopy (TEM) images of pristine Polyurethane

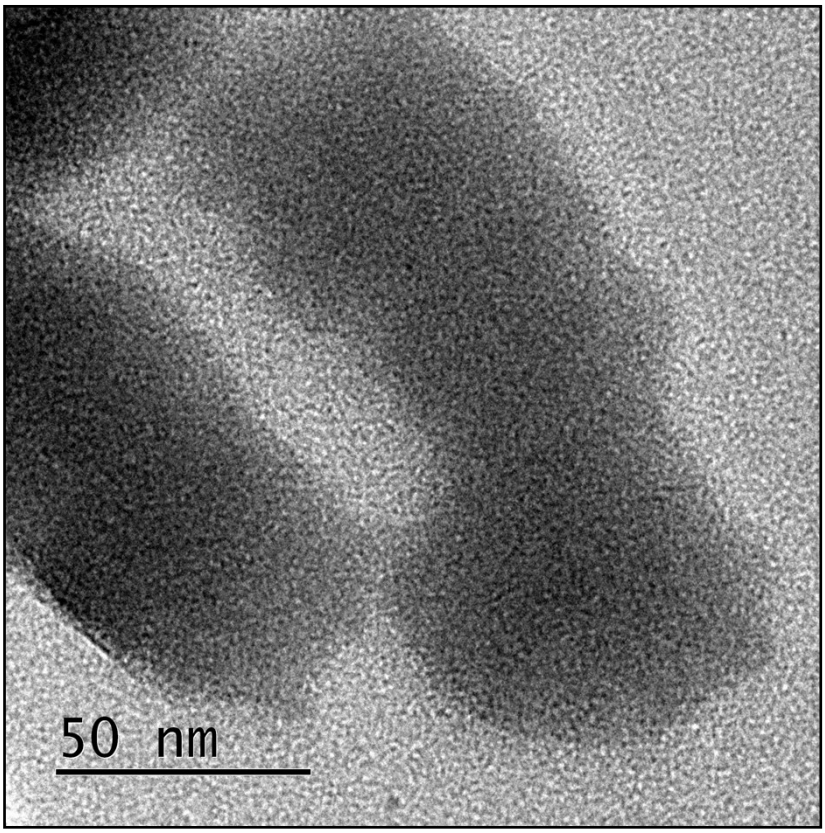

Fig S5: TEM images of ultramicrotome TPU sample where the scale bar is 50 nm.

XRD and FT-IR spectra of the pristine and nanocomposite PU after treatment with enzyme

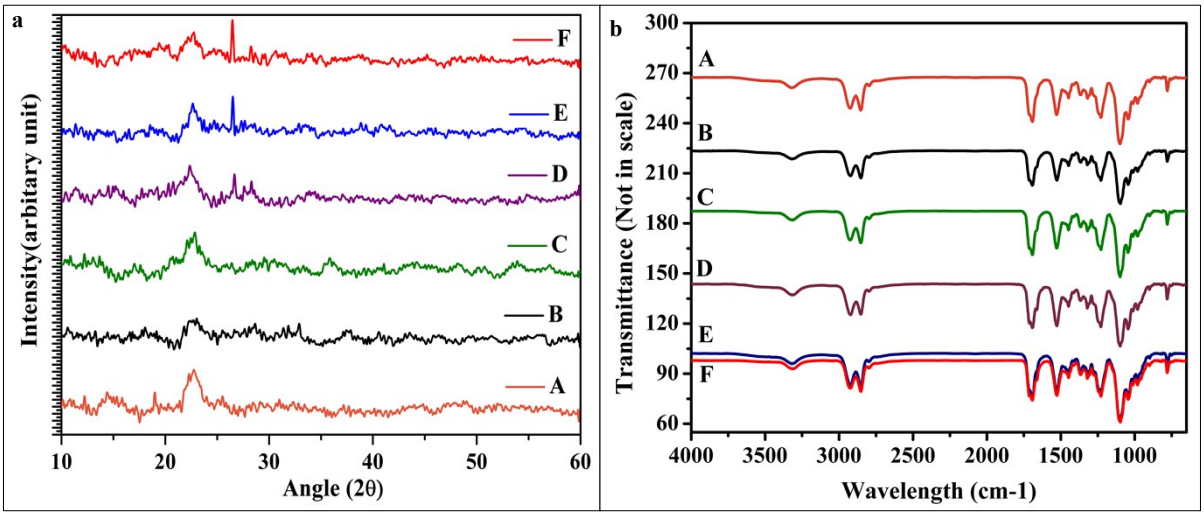

Fig S6: Figures a & b represent the XRD and FT-IR spectra of the starting PU (A) and after treatment with enzyme for 48 hrs. of PU (B), PU with 1 wt% reinforced CNP (C), CNT (D), graphene (E) and 3D hierarchical geometries (F) respectively.

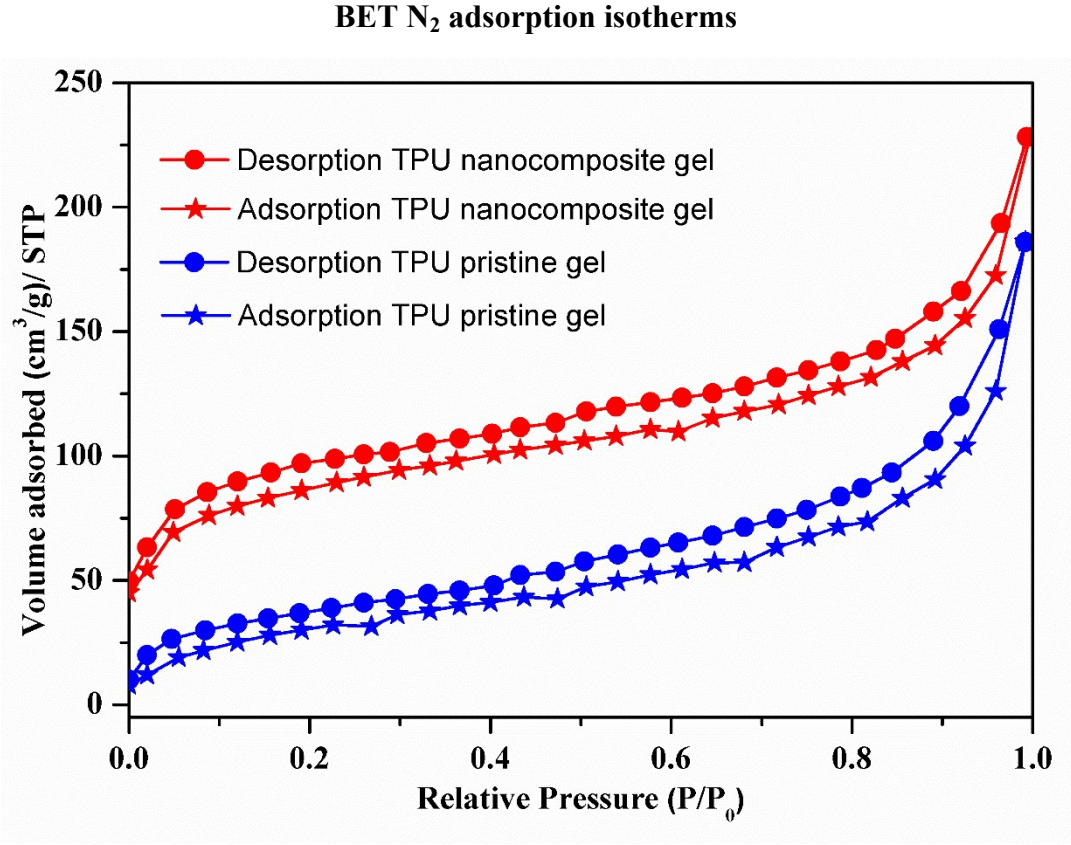

Fig S7: The comparative N_2 adsorption and desorption isotherm for TPU pristine gel (blue stars and blue circles respectively) and nanocomposite TPU gel with 1 wt% addition of hybrid nanofillers (red stars and blue circles respectively) are represented.

Zeta potentials for isoelectric points of functionalized nanomaterials

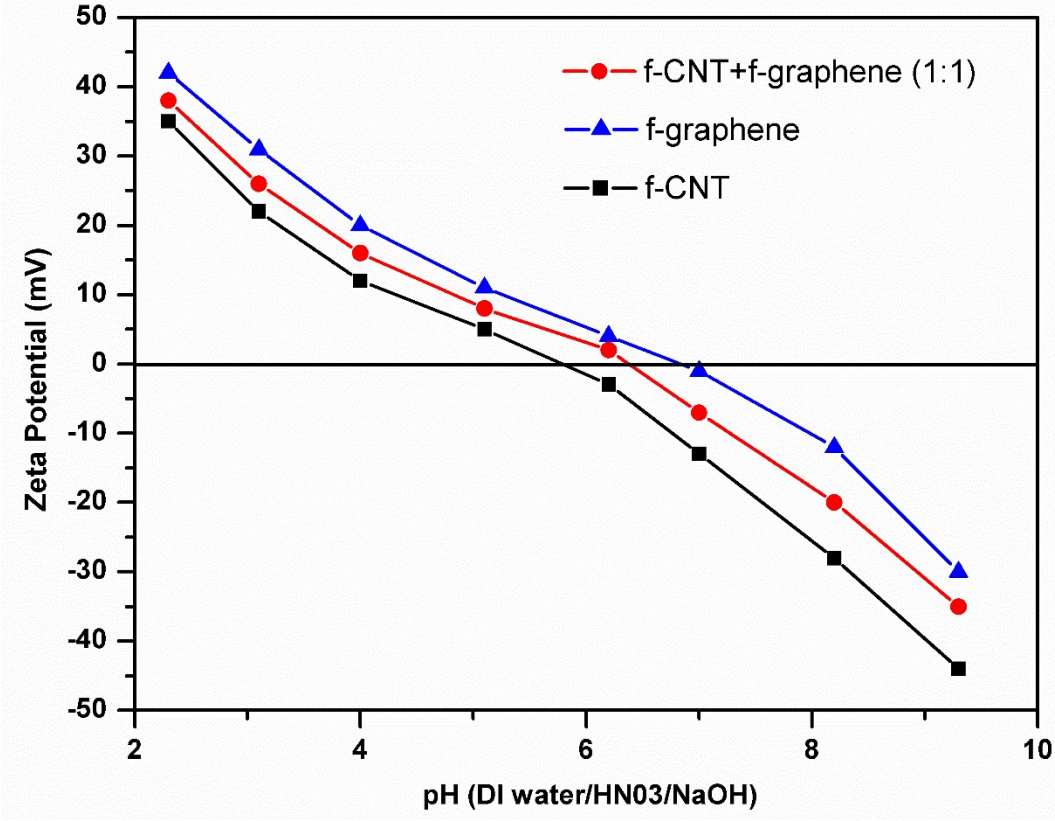

Fig S8: The point of zero charge of acid functionalized MWCNTs (black diamonds), hydroxylated graphenes (blue triangles) and f-MWCNTs embedded in to graphene flakes (1:1) (red circles) were measured by zeta potentials as a function of pH.

Fluorescence intensities with time at low concentration of different metal ions

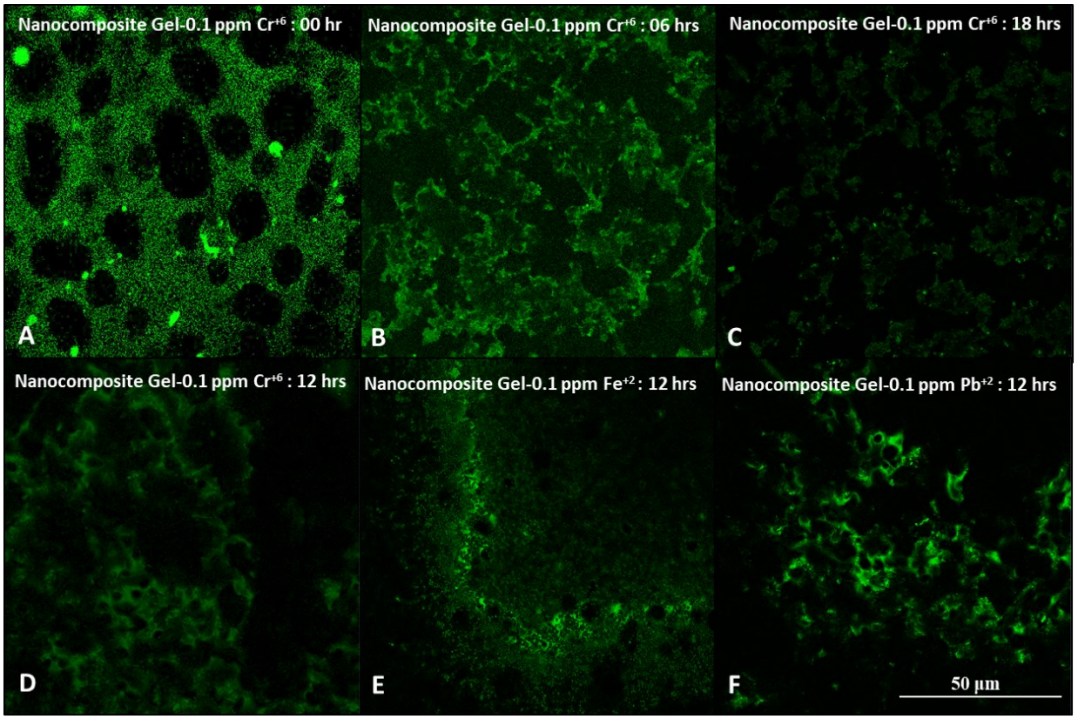

Fig S9: Fluorescence images of TPU nanocomposite gel before (A) and after treatment of 0.1 ppm chromium ions for 06 hrs (B), 12hrs (D) and 18hrs (C). The treatment of 0.1 ppm iron (E) and lead (F) ions on TPU nanocomposite gels for 12hrs are represented. The samples were dried and fixed on a glass slide with a drop of epoxy glue and viewed under an epi-fluorescence microscope by excitation at 488 nm where the scale bar is 50 µm.

UV-VIS intensities with wavelengths of different functionalized carbon nanomaterials

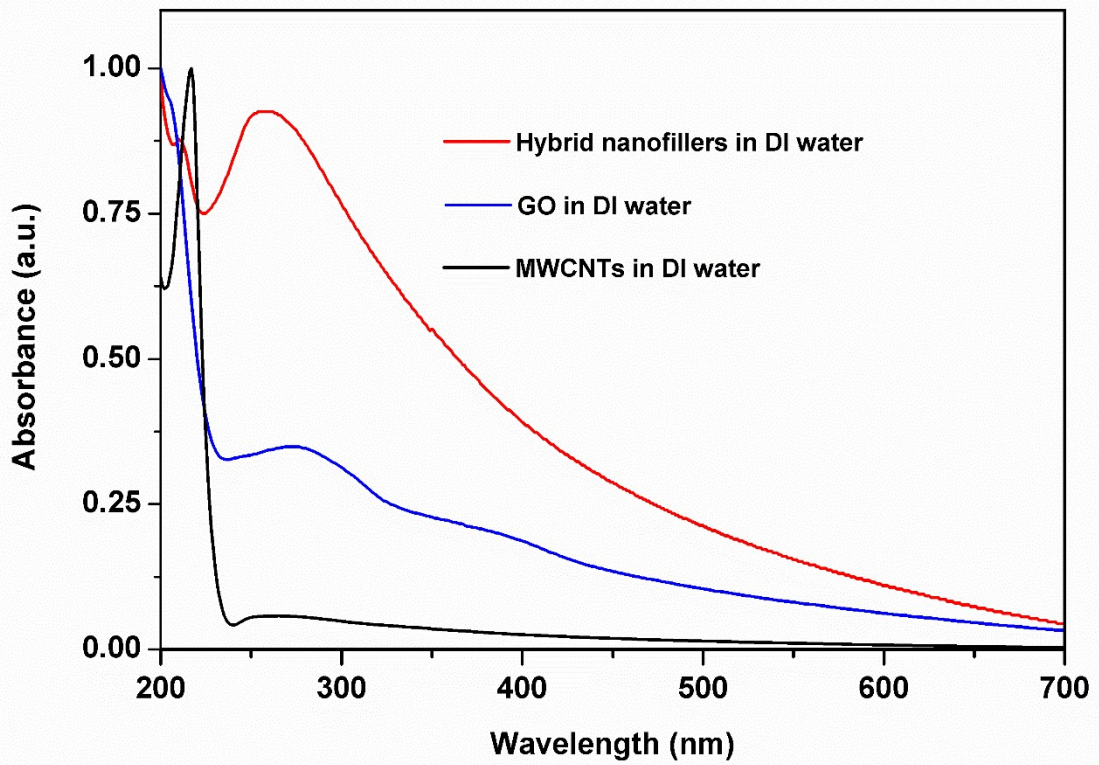

Fig S10: UV-VIS absorbance of acid functionalized MWCNTs (black line), hydroxylated graphenes (blue line) and f-MWCNTs embedded in to graphene flakes (1:1) (red line) were measured as a function of wavelength at 0.01 mg/ml concentration in DI water.